MSc in Photonics

PHOTONICSBCN

Universitat Politècnica de Catalunya (UPC)
Universitat Autònoma de Barcelona (UAB)
Universitat de Barcelona (UB)
Institut de Ciències Fotòniques (ICFO)

http://www.photonicsbcn.eu

Master in Photonics

MASTER THESIS WORK

Work analysis of one-dimensional driven quantum systems

Maria Arazo Sánchez

Supervised by Prof. Bruno Juliá Díaz and Prof. Artur Polls Martí, (UB)

Presented on date 6th September 2018

Registered at

Escola Tècnica Superior d'Enginyeria de Telecomunicació de Barcelona

Work analysis of one-dimensional driven quantum systems

Maria Arazo Sánchez

Departament de Física Quàntica i Astrofísica, Facultat de Física, Universitat de Barcelona, Martí i Franquès 1, Barcelona 08028, Spain

E-mail: `maria.arazo@gmail.com`

Abstract. We introduce the probability distribution of work performed on a one-dimensional quantum system and study the cases of a single particle in a harmonic or finite well potential and of a Bose-Einstein condensate in a finite well potential. The irreversible work is generalised for the case of Bose-Einstein condensates, described in the mean-field theory by the Gross-Pitaevskii equation. The properties of the ground state are analysed for each case, finding two different static regimes for the finite well potential (with a third one for a BEC with attractive interactions) and one for the harmonic well. Finally, the irreversible work is studied for a linear ramping protocol where the potential is widened, and a relation between the static regimes and the dynamics of the system is identified. The evolution of the system is obtained by numerically solving either the time-dependent Gross-Pitaevskii or Schrödinger equation through the Crank-Nicolson method.

Keywords: quantum work, time-dependent potential, adiabatic process, instantaneous quench, Bose-Einstein condensates.

1. Introduction

From the formalisation of the principles of the theory to the development of quantum technologies, the field of quantum physics has evolved dramatically in the last century. A common goal of both fundamental and applied research in this field is to refine the ability to control quantum systems and to tailor their dynamic evolution. Recently, this has given rise to an interest in the thermodynamics of small systems, in particular, in defining the concept of work performed on a quantum system, a magnitude that is not easily translated from classical physics.

Work is not an observable, unlike energy or position, so it cannot be associated to an operator [1, 2, 3]. A useful alternative is to define work as a random variable, W, distributed according to the work probability distribution, $P(W)$ [4]. In this stochastic definition of work, two sources of randomness arise: the thermal noise associated to the preparation of the initial state and the quantum randomness inherent in the measurement process. Therefore, work does not characterise an instantaneous state of a system but its whole evolution process. In this definition of quantum work, a system described by the Schrödinger equation is let to evolve according to a time-dependent Hamiltonian that follows a certain protocol. The concept of work and its fluctuations have been studied in several quantum systems in this framework, such as a single particle confined in a time-dependent harmonic oscillator [5] or a bosonic gas in a double well potential [6], and an experimental setup has been proposed for measuring work in ultracold quantum systems [7]. A concern to minimise the irreversible work performed during the process has lead to explore a huge variety of protocols from which shortcuts to adiabaticity stand out for their efficiency. This kind of protocols has been studied, for instance, in harmonic [8, 9] and square [10] traps.

The aim of this work is to analyse the irreversible work performed on a quantum system as we increase the size of the confining potential. We consider first a single particle trapped in either a harmonic or a finite square well potential, and propose a generalisation of the quantum work defined in [4] to study systems that evolve under a non-linear Schrödinger equation such as Bose-Einstein condensates (BECs) confined in a finite square well. Both the ground state and the evolution of the system are calculated numerically: the ground state is obtained by diagonalisation of the Hamiltonian (single particle) or using the imaginary time method (BECs), and the time evolution of the system is obtained by numerically solving the corresponding equation with the Crank-Nicolson method.

Section 2 provides general definitions of the work probability distribution and its derived quantities (average and irreversible work), and the adiabatic and instantaneous quench limits are introduced. In section 3 we describe the first system that is studied, which is a single particle trapped in a time-dependent finite well or harmonic potential, and then we introduce BECs confined in a time-dependent finite well potential, for which we generalise the concept of work proposed in [4]. In section 4, the static properties of the ground state of the system for different cases are analysed, and section 5 is devoted to the dynamics of the system when the external potential varies with time. Finally, conclusions and a brief summary are presented in section 6.

2. Work probability distribution of a quantum system

Let us consider a physical system described by a time-dependent Hamiltonian, $\hat{\mathcal{H}}(t)$, which evolves with time from $\hat{\mathcal{H}}(t_i) = \hat{\mathcal{H}}_i$ to $\hat{\mathcal{H}}(t_f) = \hat{\mathcal{H}}_f$. The initial state of the system is the ground state of the initial Hamiltonian, $\hat{\mathcal{H}}_i$, and the probability distribution function of the work performed upon the system during the evolution is defined by [1, 6]

$$P(W) = \sum_n |\langle\psi_{n,f}|\psi(t_f)\rangle|^2 \, \delta(W - E_n^f + E_0^i), \tag{1}$$

where $\{|\psi_{0,i}\rangle, E_0^i\}$ are the ground state of $\hat{\mathcal{H}}_i$ and its energy, $\{|\psi_{n,f}\rangle, E_n^f\}$ are the eigenstates and eigenvalues of $\hat{\mathcal{H}}_f$, and $|\psi(t_f)\rangle$ is the final state of the system. The

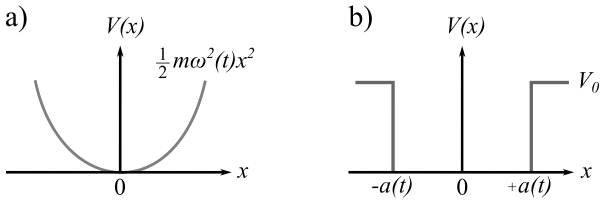

Figure 1. Trapping potentials: (a) harmonic well and (b) finite square well.

average work performed during the evolution process, $\langle W\rangle = \int W P(W)\,\mathrm{d}W$, can be obtained from (1) as the first moment:

$$\langle W\rangle = \langle\psi(t_f)|\hat{\mathcal{H}}_f|\psi(t_f)\rangle - \langle\psi_{0,i}|\hat{\mathcal{H}}_i|\psi_{0,i}\rangle, \tag{2}$$

with $\langle\psi_{0,i}|\hat{\mathcal{H}}_i|\psi_{0,i}\rangle = E_0^i$. From (2), we can define the irreversible or wasted work as

$$W_{\rm irr} = \langle W\rangle - (E_0^f - E_0^i). \tag{3}$$

Regarding the duration of the process, the two limiting scenarios are the adiabatic limit and the instantaneous quench.

Adiabatic limit. When the Hamiltonian varies slowly enough so that the system is always in the ground state of the instantaneous Hamiltonian, $\hat{\mathcal{H}}(t)$, the final state is $|\psi(t_f)\rangle = |\psi_{0,f}\rangle$. Therefore, the average work (2) for this case becomes simply the difference between the final and initial ground state energies, $\langle W\rangle = E_0^f - E_0^i$, while the irreversible work is zero.

Instantaneous quench. If $\hat{\mathcal{H}}_i$ is instantaneously changed to $\hat{\mathcal{H}}_f$, instead, the system remains on its initial state after a time t_f so that $|\psi(t_f)\rangle = |\psi_{0,i}\rangle$, and consequently the average work (2) reduces to $\langle W\rangle = \langle\psi_{0,i}|\hat{\mathcal{H}}_f|\psi_{0,i}\rangle - \langle\psi_{0,i}|\hat{\mathcal{H}}_i|\psi_{0,i}\rangle$, with a non-zero irreversible work given by (3).

3. Physical systems

3.1. Single particle in a trapping potential

The first system that will be studied is a single particle confined in an external potential, that can be either a harmonic or a finite well potential, as is schematically shown on figure 1. The system is let to evolve by varying some parameter of the external potential: the frequency ω in the case of the harmonic trap, $\frac{1}{2}m\omega^2(t)x^2$, or the halfwidth a in the case of the square trap, which is 0 if $-a(t) < x < a(t)$ and V_0 otherwise.

The evolution of the system is described by the time-dependent Schrödinger equation (TDSE) in one dimension,

$$i\hbar\frac{\partial\psi(x,t)}{\partial t} = \left[-\frac{\hbar^2}{2m}\frac{\partial^2}{\partial x^2} + V_{\rm ext}(x,t)\right]\psi(x,t), \tag{4}$$

where $V_{\rm ext}(x,t)$ is the external potential, m is the mass of the particle, $\hbar$ is the reduced Planck constant, and $\psi(x,t)$ is the wavefunction.

Two length scales of interest can be introduced. For a harmonic oscillator of frequency ω, a scale with units of distance can be defined as $\alpha = \sqrt{\hbar/(m\omega)}$. In the case of a finite well potential, besides the halfwidth a, a length scale Δ can be associated to the height of the well such that $V_0 = \hbar^2/(m\Delta^2)$, and therefore $\Delta = \hbar/\sqrt{mV_0}$.

3.2. Bose-Einstein condensates in a finite square well potential

Now we consider BECs with attractive or repulsive interactions confined in a finite well potential (figure 1b). As before, the system is let to evolve by varying the width of the well. This system is governed by the time-dependent Gross-Pitaevskii equation (TDGPE) in one dimension [11, 12] (see *Supplementary Material*),

$$i\hbar\frac{\partial\psi(x,t)}{\partial t} = \left[-\frac{\hbar^2}{2m}\frac{\partial^2}{\partial x^2} + V_{\mathrm{ext}}(x,t) + gN|\psi(x,t)|^2\right]\psi(x,t), \tag{5}$$

where N is the number of particles, the wavefunction $\psi(x,t)$ is normalised to 1, and the coupling constant $g \equiv g_{1D} = -2\hbar^2/(ma_{1D})$ [13, 14] is inversely proportional to the one-dimensional scattering length a_{1D} that characterises the interactions. Repulsive interactions occur for $g > 0$, while $g < 0$ corresponds to attractive interactions; in this work we will consider both. This equation is reduced to the TDSE (4) in the absence of interactions (*i.e.* for $g = 0$, the system is analogous to the single particle case) [15].

This system can be characterised by the two length scales considered for the single particle confined in a finite well potential, a and Δ. In the case of attractive interactions, besides these two length scales, there is a third relevant scale related to the nonlinear term known as *healing length* [16, 17], $\xi = \hbar/\sqrt{2m|g|n_0}$, where $n_0 = N|\psi(x_0,t_i)|^2$ is the central density (*i.e.* the largest density, where $x_0 = 0$) at time t_i. The healing length accounts for the size of the bright soliton that is solution of the TDGPE with no external potential, which will be introduced in section 4.

In the case of BECs, instead of using the work probability distribution, $P(W)$, we generalise the definition of the average work (2) replacing the expectation value of the Hamiltonian by the energy functional of the system at time t,

$$E_t = \int_{-\infty}^{+\infty} \mathrm{d}x\, \psi^*(x,t)\left[-\frac{\hbar^2}{2m}\frac{\partial^2}{\partial x^2} + V_{\mathrm{ext}}(x,t) + \frac{1}{2}gN|\psi(x,t)|^2\right]\psi(x,t), \tag{6}$$

so that the average work can be defined as $\langle W\rangle = E_{t_f} - E_{t_i}$, in agreement with the definition given in [18]. The irreversible work (3) thus becomes $W_{\mathrm{irr}} = E_{t_f} - E_0^f$.

4. Ground state properties

For the finite well case, we can take as units of length and time Δ and $m\Delta^2/\hbar$, so that the dimensionless variables $\tilde{x} = x/\Delta$ and $\tilde{t} = t/(m\Delta^2/\hbar)$ can be defined. Using these variables, the dimensionless TDGPE (5) can be written as

$$i\frac{\partial\tilde{\psi}(\tilde{x},\tilde{t})}{\partial\tilde{t}} = \left[-\frac{1}{2}\frac{\partial^2}{\partial\tilde{x}^2} + \tilde{V}_0 + \tilde{g}N|\tilde{\psi}(\tilde{x},\tilde{t})|^2\right]\tilde{\psi}(\tilde{x},\tilde{t}), \tag{7}$$

where the units of energy are $\hbar^2/(m\Delta^2) = V_0$ so that $\tilde{E} = E/V_0$. The dimensionless coupling constant and probability density become $\tilde{g} = g/(V_0\Delta)$ and $|\tilde{\psi}(\tilde{x},\tilde{t})|^2 = |\psi(x,t)|^2\Delta$, respectively, and the dimensionless external potential, $\tilde{V}_0$, is 0 if $-\tilde{a} < \tilde{x} < \tilde{a}$ and 1 otherwise, where $\tilde{a} = a/\Delta$. In the case of the harmonic potential, we take as units of length and time the ones corresponding to the final harmonic oscillator, α_f and ω_f^{-1}, so that the corresponding energy unit is $\hbar\omega_f$.

We consider four different cases: a single particle confined in a harmonic or square trap, and BECs with attractive or repulsive interactions confined in a square trap. Although the ground state of a single particle in the case of the harmonic oscillator can be found analytically [19] and for the finite well there is a semi-analytical solution [19], we will obtain it numerically in all cases for simplicity, since in the case of BECs there is no analytical stationary solution of the GPE. The homogeneous case (*i.e.* with no external potential) for attractive interactions is one exception, since the GPE has a solution with solitonic properties known as a *bright soliton* [11]. The stationary solution of a BEC with attractive interactions confined in a finite square well potential tends to this analytical solution as the interaction strength grows (see *Supplementary Material*).

For the cases described by the Schrödinger equation (single particle), all the eigenstates and eigenenergies are obtained by numerically diagonalising the Hamiltonian. In the presence of interactions, the ground state is found with the imaginary time method [20] (see *Supplementary Material*). All the numerical calculations have been done considering a grid of length $2L$ discretised with step Δx.

4.1. Central density for the finite well potential

We will now consider how the central density of the ground state, $\tilde{n}_0 = N|\tilde{\psi}(\tilde{x}_0)|^2$, changes with the halfwidth of the well, $\tilde{a}$, and with the healing length, $\tilde{\xi}$ (in the presence of attractive interactions). In figure 2, $\tilde{n}_0$ is plotted as function of $\tilde{a}$ for three values of the interaction. It can be seen that increasing $|\tilde{g}N|$ (*i.e.* $\tilde{\xi}$ decreases) shifts the maximum in $\tilde{n}_0$ towards lower $\tilde{a}$ for attractive interactions, since the wavefunction is narrower. For repulsive interactions the opposite occurs: the maximum goes to higher values of $\tilde{a}$ because the wavefunction is wider. This shift of the maximum is more noticeable for the case with attractive interactions. Three regimes can be defined:

Regime I. $\tilde{n}_0$ increases with increasing $\tilde{a}$,

Regime II. $\tilde{n}_0$ decreases with increasing $\tilde{a}$, and

Regime III. $\tilde{n}_0$ remains constant as $\tilde{a}$ increases.

Thus the value of $\tilde{a}$ at which $\tilde{n}_0$ is maximum determines the boundary between regimes I and II. Regime III is only observed in the case of attractive interactions, and occurs when the healing length $\tilde{\xi}$ is much smaller than the width of the well. Then, the well is big enough for the condensate to be unaffected by changes in the width of the well.

For the case of a single particle in a harmonic oscillator, there is only one length scale, α, and n_0 always decreases as the well is widened (*i.e.* the frequency, ω, decreases),

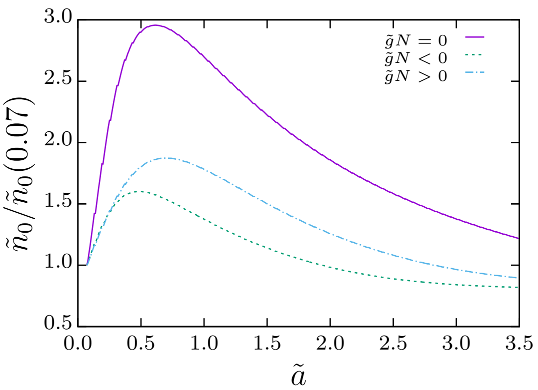

Figure 2. Central density as function of $\tilde{a}$ for: ($\tilde{g}N = 0$) single particle, ($\tilde{g}N < 0$) attractive interactions with $\tilde{g}N = -1$ and $\tilde{\xi}_m = 0.84$, and ($\tilde{g}N > 0$) repulsive interactions with $\tilde{g}N = 1$, where $\tilde{\xi}_m$ is the healing length for the maximum in $\tilde{n}_0$. In all cases, $\tilde{L} = 8$ and $\Delta\tilde{x} = 0.01$, the potential is a finite well with halfwidth $\tilde{a} \in [0.07, 3.5]$, and $\tilde{n}_0$ is normalised to $\tilde{n}_0(0.07)$, the value of $\tilde{n}_0$ when $\tilde{a} = 0.07$.

which is equivalent to regime II. If instead the particle is confined in a finite well potential, that is characterised by two lengths, Δ and a, a second regime (I) appears. Taking the limit case of the infinite well, when $\Delta \to 0$, regime I disappears.

5. Irreversible work with linear ramping

In order to study the dynamics of the system, we consider the halfwidth of the finite well to vary linearly over time from a_i to a_f as $a(t) = a_i + (a_f - a_i)t/t_f$, where $t \leq t_f$. In the case of the harmonic oscillator, the frequency $\omega(t)$ is varied from ω_i to ω_f in an analogous fashion, as it is done in [6].

The evolution of the initial state is obtained by solving the TDSE (single particle) or TDGPE (BECs) with the Crank-Nicolson method (see *Supplementary Material*). The irreversible work at the end of the process is calculated numerically according to (3) and the corresponding definition of the average work. For all the results we consider a time step $\Delta\tilde{t} = 0.001$ and perform 20000 time steps.

5.1. Definition of the dynamical regimes

Two regimes can be distinguished in the dynamics of the system: the adiabatic regime, for slow processes, which tends to the adiabatic limit as $t_f \to \infty$; and the instantaneous regime, for fast processes, that tends to the instantaneous quench if $t_f \to 0$. These regimes and the transition between them can be defined in terms of the velocities that characterise the process: the velocity associated to the mean kinetic energy at time t_i (initial velocity), and the velocity of variation of the potential (process velocity).

Initial velocity. We define it as $v_i = \sqrt{2E_{\mathrm{kin},i}/m}$, where the expectation value of the initial kinetic energy, $E_{\mathrm{kin},i}$, is calculated numerically as $-\hbar^2\langle\psi_{0,i}|\partial_x^2|\psi_{0,i}\rangle/(2m)$. This initial velocity shows a similar behaviour with respect to $\tilde{a}$ as $\tilde{n}_0$ (figure 2).

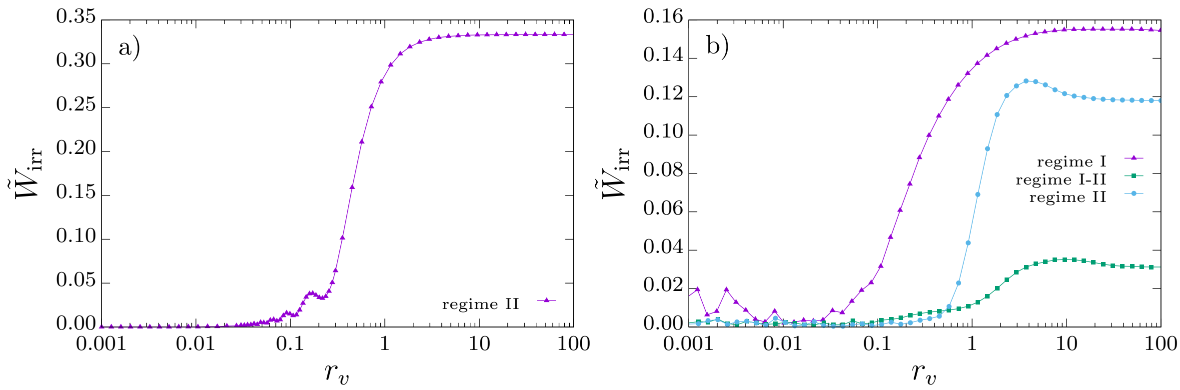

Figure 3. Irreversible work as function of the ratio of velocities, r_v. (a) Single particle in a harmonic oscillator with $\tilde{L} = 4$, where $\tilde{\omega}$ is varied from $\tilde{\omega}_i = 3.0$ to $\tilde{\omega}_f = 1.0$ and the process occurs in the static regime II. (b) Finite well with $\tilde{L} = 8$, where the initial and final $\tilde{a}$ are: (regime I) $\tilde{a}_i = 0.07$ and $\tilde{a}_f = 0.5$, (regime I-II) $\tilde{a}_i = 0.5$ and $\tilde{a}_f = 1.1$, and (regime II) $\tilde{a}_i = 1.1$ and $\tilde{a}_f = 3.2$. In all cases $\Delta\tilde{x} = 0.02$ and $r_v \in [0.001, 100]$.

Process velocity. The velocity at which the walls separate is $v_p = (a_f - a_i)/t_f$, and is analogously defined for the harmonic oscillator using the length scale α.

The ratio of these two velocities, $r_v = v_p/v_i$, determines the dynamic regimes. When the process velocity is much larger than the initial velocity ($r_v \gg 1$) we are in the instantaneous regime, whereas for small ratios ($r_v \ll 1$) the process corresponds to the adiabatic regime. The transition between the two regimes takes place when $v_p \sim v_i$.

In the following subsections we will consider a system that undergoes a certain process —for particular values of a_i and a_f (ω_i and ω_f) of the square (harmonic) trap—, and study the dynamics for different velocities of the process (*i.e.* different final times).

5.2. Single particle confined in an external potential

The irreversible work, $\tilde{W}_{\rm irr}$, for the case of a single particle trapped in a harmonic oscillator (figure 3a, with $\tilde{W}_{\rm irr} = W_{\rm irr}/\hbar\omega_f$) for different processes is first considered. For the finite well potential (figure 3b, with $\tilde{W}_{\rm irr} = W_{\rm irr}/V_0$), three cases which belong to different static regimes are studied: a case that occurs entirely in regime I, a second case that starts in regime I and ends in II, and a last case that takes place in regime II.

In figure 3a we can clearly see the adiabatic regime when $r_v \ll 1$, for which the irreversible work tends to zero. When $r_v < 1$, the irreversible work increases rapidly for larger ratios, r_v, until it reaches a constant value, which corresponds to the instantaneous regime. In order to study the dynamic regimes observed in figure 3b with more detail, we discuss the dynamics of four different ratios, r_v. Figure 4 shows, for these different cases, the evolution of the kinetic energy, $\tilde{E}_{\rm kin}$, the variance of $\tilde{x}$, $\Delta\tilde{x}^2 = \langle\tilde{x}^2\rangle - \langle\tilde{x}\rangle^2$, and the probability density that falls inside the walls, $\int_{|\tilde{x}|>\tilde{a}} |\tilde{\psi}(\tilde{x},\tilde{t})|^2 {\rm d}\tilde{x}$.

From the definition of work (2), it can be seen that the kinetic term is crucial to the calculation of the average and irreversible work, while the potential term has a minor contribution due to the fact that only the tails of the wavefunction enter the walls, where

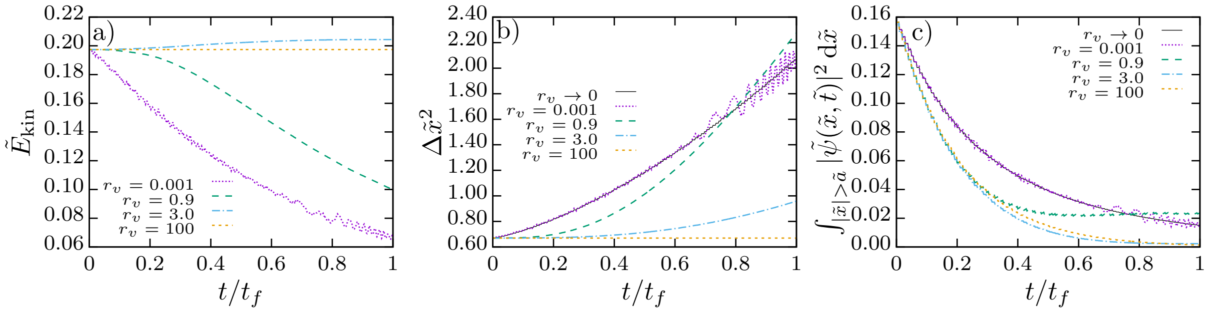

Figure 4. Evolution of the (a) kinetic energy, (b) variance of $\tilde{x}$ and (c) probability density inside the walls considering four different final times with $r_v = \{0.001, 0.9, 3.0, 100\}$ for a single particle in a finite well potential with walls moving from $\tilde{a}_i = 1.1$ to $\tilde{a}_f = 3.2$ (static regime II, figure 3b) and numerical parameters $\tilde{L} = 8$ and $\Delta\tilde{x} = 0.02$. Note that case $r_v = 0.001$ tends to the adiabatic limit ($r_v \to 0$), plotted in (b) and (c) with a black solid line.

the potential is not zero. Therefore, an increase in the kinetic energy is translated to an increase of the work performed during the process.

In general terms, we can see in figure 4 that, as the walls of the wells separate, the wavefunction broadens (*i.e.* $\Delta\tilde{x}^2$, which informs of the width, increases) and the probability density inside the walls (for $|\tilde{x}| > \tilde{a}$) decreases. Consequently, the kinetic energy decreases except in some particular situations that will be discussed below.

For instantaneous processes ($r_v \gg 1$), the system stays in the initial state: the width remains constant (and so does the kinetic energy) and the probability density inside the walls drops to zero as the walls separate. For adiabatic processes ($r_v \ll 1$), on the other hand, the wavefunction broadens as the walls separate so that the probability density inside the walls decreases more slowly; therefore, the kinetic energy decreases more than in faster processes.

There is a singular behaviour that appears for the finite well but not for the harmonic trap: if the process velocity is not much larger than the initial velocity, the walls separate at such a rate that the tails of the wavefunction bounce off of the walls instead of entering the walls, which increases the kinetic energy. This leads to an extra increase in the irreversible work that gives rise to the peak in the instantaneous regime that can be observed in figure 3b (case $r_v = 3.0$ in figure 4). Furthermore, we can see in figure 3b that the peak appears clearly for the regime II case, more faintly in regime I-II case, and is not present in the regime I case. Therefore, we finish this discussion by noting how the dynamics of the system can be characterised by the static regimes.

5.3. Effect of the non-linearity: BEC confined in a finite square well potential

Let us now consider the irreversible work, $\tilde{W}_{\text{irr}} = W_{\text{irr}}/V_0$, performed on a BEC for attractive (figure 5a) and repulsive (figure 5b) interactions where the confining potential is a finite well of varying width. As before, three cases that belong to the different static regimes are considered: one for regime I, one that starts in regime I and ends in II, and

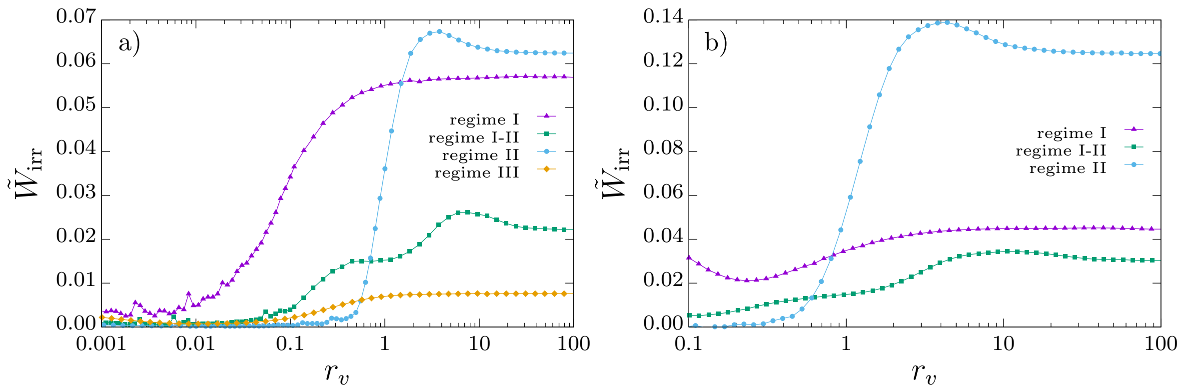

Figure 5. Irreversible work as function of the ratio of velocities, r_v, for a BEC in a finite well with (a) attractive and (b) repulsive interactions. (a) $\tilde{g}N = -2.3$ with $\tilde{L} = 4$, $\Delta\tilde{x} = 0.01$ and $r_v \in [0.001, 100]$, where $\tilde{a}_i$ and $\tilde{a}_f$ are: (regime I) $\tilde{a}_i = 0.07$ and $\tilde{a}_f = 0.22$, (regime I-II) $\tilde{a}_i = 0.22$ and $\tilde{a}_f = 0.71$, (regime II) $\tilde{a}_i = 0.71$ and $\tilde{a}_f = 2.5$, and (regime III) $\tilde{a}_i = 2.5$ and $\tilde{a}_f = 3.2$. (b) $\tilde{g}N = 0.2$ with $\tilde{L} = 8$, $\Delta\tilde{x} = 0.02$ and $r_v \in [0.1, 100]$, where $\tilde{a}_i$ and $\tilde{a}_f$ are: (regime I) $\tilde{a}_i = 0.07$ and $\tilde{a}_f = 0.42$, (regime I-II) $\tilde{a}_i = 0.42$ and $\tilde{a}_f = 1.0$, and (regime II) $\tilde{a}_i = 1.0$ and $\tilde{a}_f = 3.0$.

one for regime II. In the case of attractive interactions, a fourth case that takes place in regime III is considered.

The results for attractive (figure 5a) and repulsive (figure 5b) interactions show a similar behaviour to that of the single particle case (figure 3): two differentiated regimes with a transition in between, with a peak, surpassing the instantaneous quench, which is sharper in regime II than in the transition I-II. The new case that appears for attractive interactions (regime III) resembles that of regime I but with a much smaller variation between the two limits because the system is practically unaffected by the variation of the potential. It can be seen that the irreversible work becomes zero in the adiabatic limit ($r_v \ll 1$), as expected, except in the case of repulsive interactions for regime I.

6. Summary and conclusions

In this work, we have studied the irreversible work performed on a one-dimensional quantum system governed by the time-dependent Schrödinger equation and generalised it for systems which evolution is described by the time-dependent Gross-Pitaevskii equation. We have concentrated on the cases of a single particle in either a harmonic or a finite well potential and a BEC in a finite well in order to analyse the effects of the interactions. For the four cases, both the static and dynamic properties were studied.

Concerning the static properties, we have described how under certain conditions, in a somehow counterintuitive way, the condensate density increases at the centre when the finite well is opened. This allowed us to define two different regimes according to whether the central density increased or decreased with the halfwidth of the well. For a single particle in a harmonic potential, characterised by a single length scale, only one regime is observed, while a second one appears for a finite well potential, described by two length scales. In the case of a BEC with attractive interactions in a finite well potential, where three length scales characterise the system, a third regime —with constant central density— is observed.

Then, we have studied the evolution of the system when the width of the confining potential is increased linearly with time at different speeds. We have identified two velocities, the initial and process velocity, that allow us to characterise the main dynamical regimes that appear in the problem. The irreversible work performed during the process for different final times has been calculated in order to study the adiabatic limit and the instantaneous quench, and explore all the cases in between. We have seen that, for the finite well potential and not for the harmonic oscillator, a peak above the instantaneous quench appears on the irreversible work for some cases. Furthermore, we have been able to relate the behaviour of the irreversible work for different processes with the static regime in which the process takes place.

Possible future research could be to consider quantum engines with Bose-Einstein condensates, where the process studied here could be a part of a thermodynamic cycle.

Aknowledgements

I would like to thank Bruno Juliá and Artur Polls for their guidance throughout the project. I am also grateful to Eulàlia Nicolau and Eric Arazo for reading this manuscript.

References

[1] P. Talkner, E. Lutz, and P. Hänggi, Physical Review E **75**, 050102 (2007).
[2] M. Campisi, P. Hänggi and P. Talkner, Reviews of Modern Physics **83**, 771 (2011).
[3] P. Talkner and P. Hänggi, Physical Review E **93**, 022131 (2016).
[4] C. Jarzynski, H. T. Quan, and S. Rahav, Physical Review X **5**, 031038 (2015).
[5] S. Deffner and E. Lutz, Physical Review E **77**, 021128 (2008).
[6] R. G. Lena, G. M. Palma and G. De Chiara, Physical Review A **93**, 053618 (2016).
[7] G. De Chiara, A. J. Roncaglia, and J. P. Paz, New Journal of Physics **17**, 035004 (2015).
[8] X. Chen, A. Ruschhaupt, S. Schmidt, A. Del Campo, D. Guéry-Odelin and J. G. Muga, Physical Review Letters **104**, 063002 (2010).
[9] D. Guéry-Odelin and J. G. Muga, Physical Review A **90**, 063425 (2014).
[10] A. Del Campo and M. G. Boshier, Scientific Reports **2**, 648 (2012).
[11] L. Pitaevskii and S. Stringari, *Bose-Einstein Condensation*, (Clarendon Press, Oxford, 2003).
[12] P. G. Kevrekidis, D. J. Frantzeskakis, and R. Carretero-González, *Basic Mean-Field Theory for Bose-Einstein Condensates*, (Springer, Heidelberg, Berlin, 2008).
[13] R. Carretero-González, D. J. Frantzeskakis, P. G. Kevrekidis, Nonlinearity **21**, R139–R202 (2008).
[14] G. E. Astrakharchik, Ph.D. thesis, Università degli Studi di Trento, (2004).
[15] J. Rogel-Salazar, European Journal of Physics **34**, 247 (2013).
[16] C. Wang, Ph.D. thesis, University of Oxford, (2011).
[17] A. J. Leggett, Reviews of Modern Physics **73**, 307 (2001).
[18] J. Li, T. Fogarty, S. Campbell, X. Chen, and T. Busch, New Journal of Physics **20**, 015005 (2018).
[19] D. J. Griffiths, *Introduction to Quantum Mechanics*, (Pearson Prentice Hall, New Jersey, 2005).
[20] P. Bader, S. Blanes, and F. Casas, The Journal of Chemical Physics **139**, 124117 (2013).